Influence of Conduit Angles on Hemodynamics of Modified Blalock-Taussig Shunt: Computational Analysis of Patient-Specific Virtual Procedures

Jinlong Liu[1,*], Qi Sun[1], Mitsuo Umezu[2], Yi Qian[3], Haifa Hong[1], Zhou Du[1], Qian Wang[4], Yanjun Sun[1], and Jinfen Liu[1]

[1] Department of Cardiothoracic Surgery, Shanghai Children's Medical Center, Shanghai Jiao Tong University School of Medicine, 1678 Dongfang Road, 200127, Shanghai, China
[2] Center for Advanced Biomedical Sciences, TWIns, Waseda University, TWIns 03C-301, ASMeW Lab, 2-2 Wakamatsucho, Shinjuku 162-8480, Tokyo, Japan
[3] Australian School of Advanced Medicine, Macquarie University, North Ryde 2109, Sydney, NSW, Australia
[4] Department of Medical Imaging, Shanghai Children's Medical Center, Shanghai Jiao Tong University School of Medicine, 1678 Dongfang Road, 200127, Shanghai, China
liujinfen2007@aliyun.com

Abstract. Currently, the modified Blalock-Taussig (mB-T) shunt is the most preferred surgery served as the first step of the staged procedures in the treatment of cyanotic congenital heart defect. A Gore-Tex conduit is used to surgically connect the systemic and pulmonary circulations. In the present study, we report on three-dimensional (3D) hemodynamic analysis of the effects of conduit anastomosis angles on hemodynamics of the mB-T shunt. We constructed a patient-specific 3D model after the mB-T shunt based on medical images and employed computer-aided design to reconstruct two new models with different anastomosis angles. The local pressure, blood flow distribution and wall shear stress were calculated. The results suggest the scheme of vertical anastomosis angle of the conduit on the pulmonary artery can increase the blood flow distribution from systemic circulation to two lungs and blood flows more smoothly in the conduit. The results are well congruent with our clinical experience. This indicates the numerical methods may be applied to investigate hemodynamics of the mB-T shunt for different surgical schemes.

Keywords: Modified Blalock-Taussig shunt, Computational fluid dynamics, Computer-aided Design, Hemodynamics, Congenital heart defect.

* Corresponding Author.

S. Ma et al. (Eds.): LSMS/ICSEE 2014, Part I, CCIS 461, pp. 62–71, 2014.

1 Introduction

Since Blalock and Taussig introduced the classical form of a systemic-to-pulmonary procedure with cutting off the subclavian artery in 1945 [1], various modifications have been made to improve this kind of surgical method [2]. However, a modified form of this procedure, called the modified Blalock-Taussig (mB-T) shunt, is the most preferred procedure in clinical applications over the past decades [3, 4]. It is widely used as the first-staged procedure of surgical management for the children with cyanotic congenital heart defects. The mB-T shunt is an effective procedure to increase pulmonary blood flow by the end-to-side anastomosis of the subclavian artery (or the innominate artery) and the pulmonary artery through a Gore-Tex conduit. This surgical connection allows the blood from the systemic arteries flow into the lungs to improve the oxygen saturation of the arterial blood.

The outcomes of the mB-T shunt have improved in the past years and satisfied results are achieved in clinic. However, some complications were reported due to the complex blood flow created by the systemic pulmonary connection through the conduit, including the distortion of the pulmonary arteries, formation of post-operative thrombosis and unbalanced distribution of blood flow to two lungs. These problems are partly related to the implantation of the conduit for the improper choice of anastomosis position or angles in surgeries.

Recent development of the techniques in medical image-based computational fluid dynamics (CFD) and computer-aided design (CAD) makes it possible to perform patient-specific virtual procedures to quantitatively investigate blood flow in vitro before operations. Different surgical schemes can be designed and compared for the evaluation of operative features. A series of related information of hemodynamics can be predicted in detail to help clinicians for surgical decision-making, such as pressure drop, wall shear stress (WSS), and the distribution of blood flow. Liu et al. [5] applied the method to study the hemodynamics of distal aortic arch recoarctation following the Norwood procedure to seek for the best timing of surgical repair. CAD was used to simulate seven stages of increasing stenosis and analyzed the corresponding hemodynamics by CFD calculations. Sun et al. [6] employed the technique of CAD to design different types of total cavopulmonary connections (TCPC) with dual superior venae cavae (SVC), considering different sites for anastomosis from venae cavae to pulmonary arteries (PAs), and compared hemodynamic features in these virtual operative designs by CFD analysis.

In the present study, we used the technique of medical image-based CAD to perform virtual procedures of the mB-T shunt by adjusting the angles of conduit implantation with considering patient-specific anatomical structures. Two three-dimensional (3D) vascular geometries were constructed based on the analysis of the patient's original mB-T shunt. A computational hemodynamic system that validated in our previous studies of Norwood Procedure [7, 8] was applied to perform CFD calculations and analyze the local hemodynamics. The aim of this study was not only to disclose the patient-specific hemodynamic features at the connection area of the mB-T shunt, but also to predict the potential influence of the conduit implantation angles on hemodynamics of the mB-T shunt.

2 Materials and Methods

2.1 Clinic Data Acquisition and Patient-Specific Model Generation

Clinical studies were done around the second-staged procedure with the permission of the parents of a 12-month-old child that had undergone the mB-T shunt at five months old by using a conduit of 4 mm in diameter to surgically connect the innominate artery and pulmonary artery. Protocols were approved by the local institutional review board and regional research ethics committee of Shanghai Children's Medical Center (SCMC) Affiliated Shanghai Jiao Tong University School of Medicine.

To generate the 3D geometric model of patient-specific mB-T shunt, a series of continuous 0.625 mm-thick CT images with 512×512-pixel field of view defined the anatomies of the thorax were acquired by a 16-slice multi-detector row enhanced CT scanner (Bright Speed Elite, GE Medical System, General Electric, America). Medical imaging software RealINTAGE® (KGT Co. Tokyo, Japan) compiled and reconstructed the 3D vascular geometry. Details of our method for 3D model reconstruction were reported previously [5]. Due to the pulmonary atresia of the child, only the left ventricle provided blood flow to the body through the ascending aorta (AAo). The blood in pulmonary arteries was provided by the flow distributed from the systemic circulation through a surgical implanted conduit. Fig.1 depicts the 3D reconstructed vascular geometry of the patient-specific mB-T shunt.

The mass flow at the AAo was acquired by echocardiography in real time with electrocardiogram (ECG). The distribution of blood pressure measured during the second-staged procedure at the left pulmonary artery (LPA) and the right pulmonary artery (RPA), respectively, were stored in ASCII format for CFD simulation.

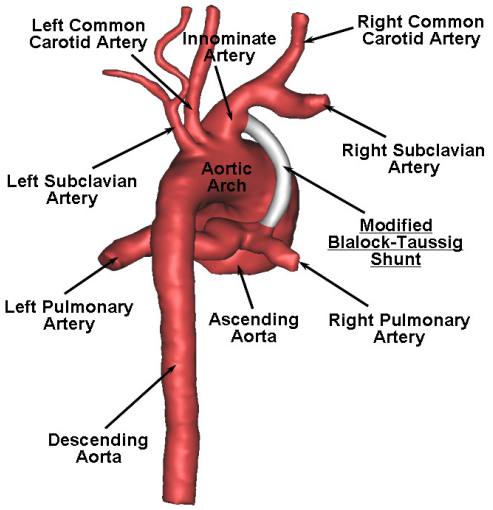

Fig. 1. Reconstruction of 3D patient-specific vascular geometry from original CT images

2.2 Model Rebuilding

Model rebuilding was done by the analysis of patient-specific anatomical structures of arteries in the mB-T shunt. To make new models, the implantation angles of conduit were adjusted based on clinical requirements considering that no kinking should be generated in the conduit. During this process, we applied the commercial software Materialise ® -Mimics 12.0 to complete the 3D geometry separation, angle modification and model reassemble. Two parameters, θ_1 and θ_2, were defined for the accurate control of the angle adjustment. The θ_1 was used to describe the angle between the innominate artery and the conduit, and θ_2 was employed to express the angle created by the anastomosis of the conduit and pulmonary artery. Two new virtual models were rebuilt for the CFD analysis in the present study, which expressed two possible surgical designs of the patient-specific mB-T shunt.

Compared with the original model, Model 1 adjusted θ_1 from 90° to 60°, and kept the same degree of θ_2. Model 2 modified θ_2 from 120° to 90°, and kept θ_1 with the same degree of the original model. We examined the patient-specific anatomical structures and found that the two models with above angles represented the two extreme conditions of conduit implantation without generating kinking in this patient. Other possible implantation angles should be in the range of 60°-90° for θ_1 and 90°-180° for θ_2 in the procedure of the patient-specific mB-T shunt. Figure 2 compared the models with the changes of anastomosis angle.

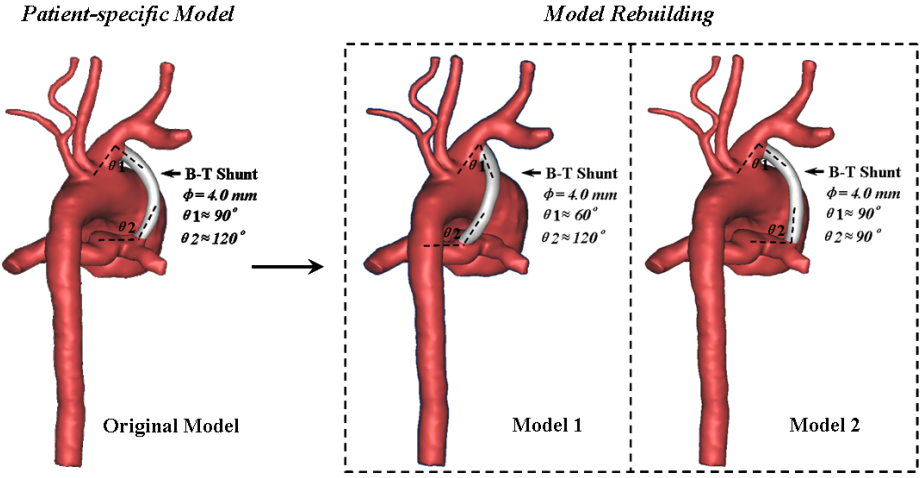

Fig. 2. Two virtual models constructed by computer-aided design with the changes of anastomosis angle

2.3 CFD Analysis

2.3.1 Governing Equations

The equations governing blood flow are the 3D incompressible Navier-Stokes (N-S) equations, which were described as below,

$$\begin{cases} \dfrac{\partial}{\partial t}(\rho u_i)+\dfrac{\partial}{\partial x_j}(\rho u_i u_j)=-\dfrac{\partial p}{\partial x_i}+\dfrac{\partial}{\partial x_j}\left[\mu\left(\dfrac{\partial u_i}{\partial x_j}+\dfrac{\partial u_j}{\partial x_i}\right)\right]+f_i \\ \dfrac{\partial \rho}{\partial t}+\dfrac{\partial}{\partial x_j}(\rho u_j)=0 \end{cases} \tag{1}$$

where i, j=1, 2, 3, x_1, x_2, and x_3, represent coordinate axes, u_i, u_j are velocity vectors, p is pressure, μ is viscosity, ρ is density, and t is time. The term f_i expresses the action of body forces.

Because arteries are large relative to individual blood cells [9] and shear rates are greater in larger arteries [10], we assumed blood to be a Newtonian fluid with constant density (ρ = 1060 kg m^{-3}) and viscosity (μ =4.0×10^{-3} Pa s) and the body forces were omitted.

We calculated the Reynolds numbers based on blood flow at the anastomosis of the mB-T shunt in one cardiac cycle, and found the maximum value was closed to 5000. Accordingly, the blood flow should be the turbulence flow in the patient-specific vascular geometry. The most widely validated turbulence model, the standard $k-\varepsilon$ model, was employed to solve the complex flows [11].

The flow distribution ratio (FDR) was defined to evaluate the balance of blood distribution between systemic and pulmonary circulations in the three models. The equation for FDR is given by:

$$FDR=\frac{Q_{outlet}}{Q_{inlet}}\times 100\% \tag{2}$$

where Q_{outlet} is the flow in the LPA, RPA, descending aorta (DA), left subclavian artery (LSA), right subclavian artery (RSA), left common carotid artery (LCCA), right common carotid artery (RCCA) and Q_{inlet} is the inflow at the AAo.

2.3.2 Mesh Generation

The grid-generation software, ANSYS®-ICEM 14.0 was applied to discretize the computational domain of the three models for CFD calculations. A combination of tetrahedral grids in the interior and five-layer body-fitted prismatic grids in the near-wall regions was employed for numerical solution of the equations governing blood motion.

To find the best mesh for CFD analysis, grid-independent verification were performed in our previous study and found that grid numbers of about one million would make the most efficient mesh in calculation of aortic flow [8]. Table 1 lists the mesh information for each model, including the patient-specific 3D model.

Table 1. Mesh information for each model

Model	Original Model	Model 1	Model 2
Total Nodes	565,394	559,954	566,504
Total Elements	1,503,964	1,490,333	1,507,513

2.3.4 Boundary Conditions

Due to the pulmonary atresia, the AAo was the only inlet of blood flowed into the arteries. To fully develop the flow boundary layer, the inlet domain was extended upstream to twenty times the size of the AAo. The pulsatile mass flow, measured by echocardiography in real-time with an electrocardiogram recorder, was imposed as the inflow conditions on the extended inlet.

At the outlet of the DA, LSA, LCCA, RCCA, and RSA, we extended sixty times of vessel diameter in a normal direction to allow sufficient recovery of blood pressure in each branch. A zero pressure gradient was used at these outlets. The estimated pressure wave reflections from peripheral vessels at diastolic phase proposed in our previous study of Norwood procedure [7] was applied to model cardiovascular flow. The pressure waves in pulmonary arteries, which were considered to be greatly affected by respiration and blood flow pulsation [12], were measured at the LPA and RPA during the patient's second-staged procedure. These profiles were imposed as the pressure outlet conditions in calculations. To avoid the influence of boundaries, we used same conditions at the inlet and outlet to predict hemodynamic features in the three models.

2.3.5 Calculation

CFD calculations were performed on the finite volume solver package, ANSYS®-FLUENT 14.0, to solve the turbulence flow inside the connection area of the mB-T shunt. For the simulation, we assumed vascular walls were rigid and impermeable, with no-slip boundary conditions. For convergence criteria, the relative variation of the quantities between two successive iterations was smaller than the pre-assigned maximum, 10^{-5}. We chose a second-order upwind scheme for discretization of the governing equations and all calculations were converged to 10^{-6}.

Simulations were run for three consecutive cardiac cycles to yield stable and precise periodic results, and the results of the last cycle were used for hemodynamic analysis.

3 Results

Fig.3 depicts the contour plots of the total pressure and WSS. Fig.3 (a) displays the results when the AAo's mass flow arrived at systolic peak. In the patient-specific model, there is a high pressure drop in the mB-T shunt at systolic peak, approximately 60 mmHg. Relatively low pressure area is observed at the connection area between the conduit and the PA. In Model 1, due to the sharp angle of θ_1, a relatively high pressure drop is found at the connection area of the IA and conduit. Compared to the patient-specific model, almost the same value of pressure drop is observed at the anastomosis of the PA and conduit. When the θ_2 changes from 120° to 90° in Model 2, the total pressure drop decreases inside the conduit. There is approximately 50 mmHg at systolic peak.

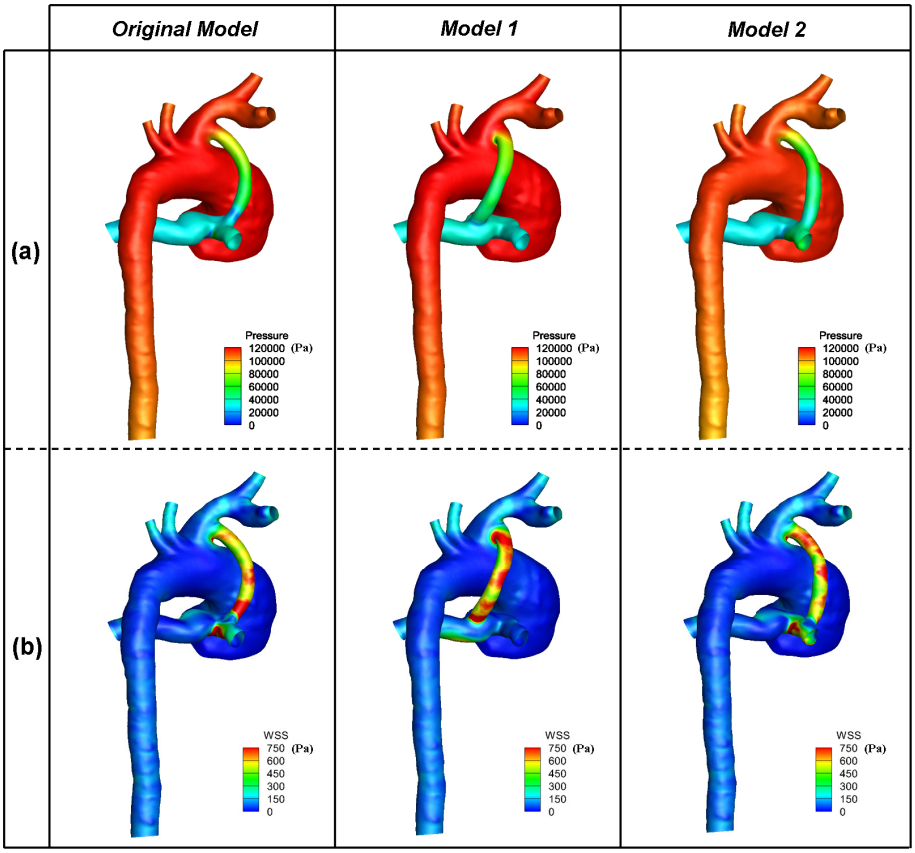

Fig. 3. The contour plots of the total pressure (a) and WSS (b) at systolic peak

WSS, as one of the most important hemodynamic indicators, is related to the remodeling process in the arterial walls and thrombosis formation. Fig.3 (b) displays the distribution of WSS. High values of WSS appear in the conduit and the orifice of the mB-T shunt at the PA in the patient-specific Model. When the θ_1 decreased from 90° to 60° in Model 1, the value of WSS increased sharply at the connection area of the IA and conduit. Large areas of high WSS distribution are observed inside the conduit in Model 1. This indicates that blood flow has accelerated and become more unstable and complex. Due to the restriction of the conduit, blood flow collides directly to the PA. High values of WSS are found at the orifice of conduit to PA. In Model 1, the areas of high values of WSS primarily located at the LPA, while they are mainly distributed at the RPA in the patient-specific model and Model 2.

We calculated the distribution ratio of mass flow at each branch. Table 2 shows these results of the three models respectively. With the decrease of the θ_1, the mass flow distributed to the PA was declined around 6% of inflow in Model 1. Blood flow to the body through the DA increased by 3.42%. The flow distribution ratios in other branches have some increase. When the θ_2 changed from 120° to 90° in Model 2, a little increase of mass flow passed through the mB-T shunt, with 45.14% of the inflow distributed to the PA and the amount of blood to the DA decreased by 2.4%.

Table 2. The proportion of blood flow distribution (%)

	Original Model	Model 1	Model 2
mB-T shunt	42	37.61	45.41
DA	45	48.42	42.6
LSA	2.5	2.69	2.26
RSA	4.2	4.53	4.01
LCCA	3	3.2	2.86
RCCA	3.3	3.55	3.13

Note: The proportion of the mB-T Shunt expresses the ratio of blood flowed into pulmonary artery passed through the conduit.

4 Discussion

Since the hearts are dysfunctional among the cyanotic CHD patients needed to perform the mB-T shunt, little pressure drop, high WSS and small changes of the blood flow distribution are all important for the survival of the suffering weak hearts and post-operative recovery. Minimizing these factors by optimizing the anastomosis configurations is crucial in the clinical practice.

In the present study, we virtually rebuilt two models by using CAD to adjust the conduit anastomosis angles based on the patient-specific vascular geometry after the procedure of the mB-T shunt. In model 1, we adjusted θ_1 to its minimum angle. The outside wall of the conduit touched the surface of AAo without a kinking created. In model 2, we modified θ_2 to 90°. The conduit was vertically anastomosed on the PA. The angle was considered the optimal angle in the procedure of mB-T shunt based on our clinical experience. The effects of the anastomotic shape, which were considered to have influence on the hemodynamics in procedure, did not take into account in the present study. We kept same anastomotic shape in the process of model rebuilding.

Studies suggested that when the value of Q_p /Q_s (where Q_p was the flow distributes to pulmonary arteries through the conduit, and Q_s was the flow distributes to systemic circulation) reached between 0.5 and 1 [13], the maximal oxygen delivery would be achieved in the systemic-to-pulmonary procedure. We calculated value of Q_p /Q_s and found they were 0.724, 0.603 and 0.823 in three models, respectively. This indicated Model 2 with the conduit vertically anastomosed on the PA can delivery more oxygen in the arterial blood to alleviate cyanosis. The result was well congruent with our clinical experience. Model 1 was the worst design when θ_1 to its minimum angle.

The understanding of pathophysiological changes in the formation of thrombosis and occlusion is critical to improve surgical design of the mB-T shunt. Studies have shown a strong correlation in the magnitude of WSS, endothelial cell function, and vessel wall remodeling [14, 15]. High WSS can damage the endothelial layer of blood vessels. Moreover, low WSS coincided with areas of low flow velocity is considered to promote platelet activation, which is one of the reasons for causing shunt thrombosis and occlusion [16]. In Model 1, relatively high WSS was observed inside the conduit and the bottom of the LPA. It meant large damage of the

endothelial layer of blood vessels may be created in the LPA when the θ_1 was decreased. Due to the change of flow direction, low WSS was generated in the RPA. Although some areas of high WSS were also found inside the conduit in patient-specific model and Model 2, the region of high WSS appeared in PA is smaller comparing to Model 1. This implied relatively small range of damage of the endothelial layer may be made in the PA. As a result, the risk of the formation of thrombosis and occlusion was reduced. Accordingly, the decline of θ_1 can increase the WSS along the conduit and the change of θ_2 can control the distribution area of high WSS in the PA.

5 Conclusion

In the present study, the technique of CAD was used to adjust the anastomosis angles between the IA or PA and the conduit to virtually simulate two different surgical schemes. By the analysis of the distribution of pressure, WSS and flow ratio, the scheme of vertical anastomosis angle of the conduit on the PA was thought to be the optimal design of the procedure to increase the blood flow distribution from systemic circulation to two lungs and blood flows more smoothly in the conduit. The results are well congruent with our clinical experience. The studies of virtual procedure and its hemodynamic analysis are helpful in the surgical design of the mB-T shunt.

6 Conflict of Interest Statement

The authors of this manuscript have no conflicts of interest to disclose.

Acknowledgment. The authors wish to thank Prof. Mitsuo Umezu and Prof. Yi Qian for many fruitful discussions and suggestions arisen during the preparation of this work. This work was supported by the National Nature Science Foundation of China (No. 81070133. P.I.: Jinfen Liu and No. 81100117. P.I.: Qi Sun), Project funded by China Postdoctoral Science Foundation (No. 2013M530200. P.I.: Jinlong Liu), and the fund of The Shanghai Committee of Science and Technology (No. 134119a3900. P.I.: Yanjun Sun).

References

1. Blalock, A., Taussig, H.B.: The Surgical Treatment of Malformations of the Heart in Which there is Pulmonary Stenosis or Pulmonary Atresia. JAMA 128, 189–202 (1945)
2. Rodríguez, E., Soler, R., Fernández, R., Raposo, I.: Postoperative Imaging in Cyanotic Congenital Heart Diseases: Part 1, Normal findings. Am. J. Roentgenol. 189, 1353–1360 (2007)
3. de Leval, M.R., McKay, R., Jones, M., Stark, J., Macartney, F.J.: Modified Blalock–Taussig shunt: Use of the Subclavian Artery Orifice as Flow Regulator in Prosthetic Systemic Pulmonary Artery Shunts. J. Thorac. Cardiovasc. Surg. 81, 112–119 (1981)

4. Garson, A., Bricker, J.T., Fisher, D.J., Neish, S.R.: The Science and Practice of Pediatric Cardiology, 2nd edn. Williams & Wilkins, Baltimore (1998)
5. Liu, J.L., Qian, Y., Itatani, K., Murakami, A., Shiurba, R., Miyaji, K., Miyakoshi, T., Umezu, M.: Image-Based Computational Hemodynamics of Distal Aortic Arch Recoarctation Following the Norwood Procedure. In: 4th International Congress on Image and Singal Processing, pp. 318–323. IEEE Press, New York (2011)
6. Sun, Q., Liu, J.L., Qian, Y., Zhang, H.B., Wang, Q., Sun, Y.J., Hong, H.F., Liu, J.F.: Computational Haemodynamic Analysis of Patient-specific Virtual Operations for Total Cavopulmonary Connection with Dual Superior Venae Cavae. European Journal of Cardio-Thoracic Surgery (2013), doi:10.1093/ejcts/ezt394
7. Liu, J.L., Qian, Y., Itatani, K., Miyakoshi, T., Murakami, A., Ono, M., Shiurba, R., Miyaji, K., Umezu, M.: An Approach of Computational Hemodynamics for Cardiovascular Flow Simulation. In: ASME-JSME-KSME 2011 Joint Fluids Engineering Conference, pp. 1449–1456. American Society of Mechanical Engineers (2011)
8. Qian, Y., Liu, J.L., Itatani, K., Miyaji, K., Umezu, M.: Computational Hemodynamic Analysis in Congenital Heart Disease: Simulation of the Norwood Procedure. Ann. Biomed. Eng. 38, 2302–2313 (2010)
9. McDonald, D.A.: Blood Flow in Arteries. Edward Arnold Ltd. (1974)
10. Fung, Y.C.: Biomechanics. Springer-Verlag (1981)
11. Launder, B.E., Sharma, B.I.: Application of the Energy Dissipation Model of Turbulence to the Calculation of Flow near a Spinning Disc. Letters in Heat Mass Transfer 1, 131–138 (1974)
12. Marsden, A.L., Vignon-Clementel, I.E., Chan, F.P., Feinstein, J.A., Taylor, C.A.: Effects of Exercise and Respiration on Hemodynamic Efficiency in CFD Simulations of the Total Cavopulmonary Connection. Ann. Biomed. Eng. 35, 250–263 (2007)
13. Barnea, O., Santamore, W.P., Rossi, A., Salloum, E., Chien, S., Austin, E.H.: Estimation of Oxygen Delivery in Newborns with a Univentricular Circulation. Circulation 98, 1407–1413 (1998)
14. Adel, M.M., Seth, L.A., Seigo, I.: Hemodynamic shear stress and its role in atherosclerosis. JAMA 282(21), 2035–2042 (1999)
15. Gimbrone, M.A., Resnick, N., Nagel, T., Khachigian, L.M., Collins, T., Topper, J.N.: Hemodynamics, Endothelial Gene Expression, and Atherogenesis. Ann. N. Y. Acad. Sci. 811(1), 1–10 (1997)
16. Odim, J., Portzky, M.D., Zurakowski, G., Wernovsky, R.P., Burke, R.P., Mayer, J.E., Castaneda, A.R., Jonas, R.A.: Sternotomy Approach for the Modified Blalock-Taussig Shunt. Circulation 92, II256–II261 (1995)